

# Identification of Chemicals that Cause Oxidative Stress in Oil Sands Process-Affected Water

Jianxian Sun,<sup>†</sup> Hui Peng,<sup>\*,†,‡,h</sup> Hattan A. Alharbi,<sup>†</sup> Paul D. Jones,<sup>†,‡</sup> John. P. Giesy,<sup>†,‡,§,||,⊥,#,▽</sup> and Steve B. Wiseman<sup>\*,h</sup>

<sup>†</sup>Toxicology Centre, University of Saskatchewan, 44 Campus Drive, Saskatoon, Saskatchewan Canada

<sup>‡</sup>School of Environment and Sustainability, 117 Science Place, Saskatoon, Saskatchewan Canada

<sup>§</sup>Department of Veterinary Biomedical Sciences, University of Saskatchewan, Saskatoon, Saskatchewan Canada

<sup>||</sup>Zoology Department, Center for Integrative Toxicology, Michigan State University, East Lansing, Michigan United States

<sup>⊥</sup>School of Biological Sciences, University of Hong Kong, Hong Kong Special Administrative Region, People's Republic of China

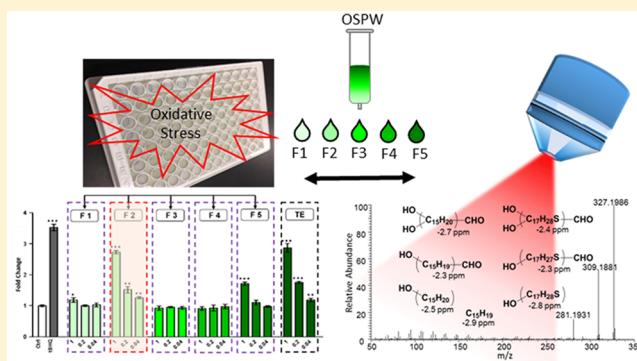
<sup>#</sup>State Key Laboratory of Pollution Control and Resource Reuse, School of the Environment, Nanjing University, Nanjing, People's Republic of China

<sup>▽</sup>Biology Department, Hong Kong Baptist University, Hong Kong, SAR, China

<sup>h</sup>Department of Biological Sciences, University of Lethbridge, Lethbridge, Alberta T1K 3M4, Canada

## Supporting Information

**ABSTRACT:** Oil sands process-affected water (OSPW) has been reported to cause oxidative stress in organisms, yet the causative agents remain unknown. In this study, a high-throughput in vitro Nrf2 reporter system was used, to determine chemicals in OSPW that cause oxidative stress. Five fractions, with increasing polarity, of the dissolved organic phase of OSPW were generated by use of solid phase extraction cartridges. The greatest response of Nrf2 was elicited by F2 ( $2.7 \pm 0.1$ -fold), consistent with greater hydroperoxidation of lipids in embryos of Japanese medaka (*Oryzias latipes*) exposed to F2. Classic naphthenic acids were mainly eluted in F1, and should not be causative chemicals. When F2 was fractionated into 60 subfractions by use of HPLC, significant activation of Nrf2 was observed in three grouped fractions: F2.8 ( $1.30 \pm 0.01$ -fold), F2.16 ( $1.34 \pm 0.05$ -fold), and F2.25 ( $1.28 \pm 0.15$ -fold). 54 compounds were predicted to be potential chemicals causing Nrf2 response, predominated by  $\text{SO}_3^+$  and  $\text{O}_3^+$  species. By use of high-resolution  $\text{MS}^2$  spectra, these  $\text{SO}_3^+$  and  $\text{O}_3^+$  species were identified as hydroxylated aldehydes. This study demonstrated that polyoxygenated chemicals, rather than classic NAs, were the major chemicals responsible for oxidative stress in the aqueous phase of OSPW.



## INTRODUCTION

Extraction of bitumen from the oil sands of Alberta, Canada has increased rapidly with projected output ranging from 2.0 to 2.9 million barrels per day by 2020.<sup>1,2</sup> In surface mining operations, extraction of bitumen from oil sands with hot water results in production of oil sands process-affected water (OSPW). Development of oil sands and leakage from tailings ponds has raised concerns about potential pollution and ecological/health risks posed by exposure to OSPW.<sup>3,4</sup> Specifically, there is concern about the rate at which OSPW in end pit lakes (EPLs) will be detoxified.<sup>5</sup> Development of tools, such as bioassays and high-resolution mass spectrometry analysis of specific chemicals that cause toxicity, to monitor detoxification of OSPW in EPLs would greatly assist industry and regulatory agencies charged with monitoring EPLs.

OSPW has been reported to cause multiple chronic toxicities,<sup>6–12</sup> but the mechanism(s) of these toxicities are not well understood. Numerous studies have suggested that oxidative stress, which can lead to damage to nucleotide acids, proteins, and lipids, and thereby cause cellular dysfunction and ultimately cause phenotypic adverse effects, might be an important mechanism of toxicity of OSPW.<sup>7,9,13</sup> In hepatocytes of rainbow trout (*Oncorhynchus mykiss*), expression of genes related to oxidative stress was significantly up-regulated after exposure to OSPW,<sup>14</sup> and oxidative stress and apoptosis were induced in embryos of fathead minnows exposed to OSPW.<sup>7</sup>

Received: April 18, 2017

Revised: June 22, 2017

Accepted: June 29, 2017

Published: June 29, 2017

Cytotoxicity in strains of yeast exposed to OSPW has also been reported to be mediated by pathways related to oxidative stress.<sup>13</sup> Results of both *in vitro* and *in vivo* experiments indicated the significance of oxidative stress as mechanism of toxicity of OSPW, but identities of those chemicals in OSPW that cause oxidative stress are not known.

Because the aqueous phase of OSPW is a complex mixture of dissolved organic compounds it is difficult to identify those chemicals that cause toxicities. Advances in ultrahigh-resolution mass spectrometry have led to understanding that the aqueous phase of OSPW contains not only naphthenic acids (NAs;  $C_nH_{2n+2}O_2$ ),<sup>15</sup> but also mono- and polyoxygenated compounds, many unidentified species of acids containing sulfur and nitrogen atoms, and a variety of polar neutral substances containing oxygen, sulfur, and nitrogen.<sup>16–18</sup> Initial studies of the toxicity of OSPW suggested that toxicity of OSPW was caused by NAs.<sup>19</sup> However, it has been argued that these studies implicate a broader group of polar organic acids as causative of the toxicity of OSPW.<sup>15,20</sup> Recently, NAs and several species of polar neutral compounds containing oxygen and sulfur were identified as causing acute lethality.<sup>11,12</sup> In another study, a pull-down assay, combined with untargeted chemical analysis (termed PUCA) was used to identify ligands of peroxisome proliferator-activated receptor  $\gamma$  (PPAR $\gamma$ ) from extracts of OSPW.<sup>21</sup> However, because oxidative stress could be mediated by multiple pathways, rather than one known target, targeted enrichment of corresponding toxic components using the PUCA assay is not available.

Effects-directed analysis (EDA) has been used extensively to identify toxic components of complex mixtures.<sup>6,22,23</sup> In the current study, a high-throughput and reproducible *in vitro* assay and high-resolution EDA were recruited for identification of causative chemicals in OSPW. The transcription factor NF-E2-related factor 2 (Nrf2) has been identified as a general regulator of cellular defense against oxidative stress through binding to the antioxidant response element (ARE) in the upstream promoter region of many genes that are important for defense against oxidative stress.<sup>24,25</sup> Elevated levels of ROS or electrophilic species that resulted in an altered redox status in cells could trigger the transcriptional response mediated by Nrf2.<sup>24,26</sup> In this study, a cell line that has been stably transfected with a pTA-NRF2-luciferase reporter vector was used as *in vitro* monitoring system, in combination with *in vivo* Medaka exposure, and untargeted chemical analysis conducted by Q Exactive quadrupole, Orbitrap, to identify chemicals in OSPW that cause oxidative stress.

## MATERIALS AND METHODS

**Chemicals and OSPW.** Hexane, dichloromethane (DCM), and methanol (MeOH), each of HPLC grade, were purchased from Fisher Scientific (Ottawa, ON, Canada). Anhydrous ethanol was obtained from GreenField Ethanol Inc. (Brampton, ON, Canada). OSPW was collected during September of 2012, from Base Mine Lake, which is the first end-pit-lake in the surface mining oil sands industry and was constructed from the West-In-Pit settling basin that received water from the main extraction facility on the site of Syncrude Canada, Ltd. (Fort McMurray, AB, Canada). The OSPW was shipped to the University of Saskatchewan (Saskatoon, SK, Canada), stored in the dark, and used for fractionation immediately upon arrival.<sup>21,27</sup>

**OSPW Fractionation.** A 500 mg EVO-LUTE ABN solid phase extraction (SPE) cartridge (Biotage, Charlotte, NC) was

used for initial extraction and fractionation of organic chemicals in the aqueous phase of OSPW. This adsorbent material was used because initial experiments showed that this cartridge could capture more constituents of OSPW than did HLB cartridges.<sup>19</sup> A procedure blank was conducted using ultrapure water, and no significant Nrf2 activity was detected. Prior to fractionation, to remove particulate matter, 1 L of OSPW was passed through a glass microfiber filter (GF/D 0.47 mm, Whatman) then pH was adjusted to 2 by use of concentrated HCl (37%). Cartridges were conditioned with 6 mL of methanol and 6 mL of pure water and a 1 L aliquot of filtered and acidified OSPW was passed through cartridges, which were subsequently washed with water and allowed to dry under vacuum for 30 min. Fractionation, based on polarity, was used to separate constituents of OSPW into five fractions isolated with successive mixtures of solvents of increasing polarity. Fractions were eluted with 6 mL of solvents (volume percentage, v/v) in sequence as follows (Supporting Information (SI) Figure S1): F1) 100% Hexane; F2) 20% DCM in hexane; F3) 50% DCM in hexane; F4) 100% DCM; and F5) 100% MeOH. Fractions were dried under nitrogen and redissolved in 500  $\mu$ L of ethanol to get a final 2000 $\times$  nominal concentration of original OSPW sample. The distribution of each chemical specie across SPE fractions has been described in our previous study.<sup>21</sup> Equal volumes of the five fractions were pooled to make a reconstituted total extract (TE) of dissolved organic chemicals from OSPW. Recoveries of OSPW compounds were determined by comparing the relative abundance of species in original OSPW water and OSPW extracts eluted from SPE cartridges. The recoveries were ranged from 30.9% ( $SO_4^{+}$ ) to 143% ( $O_5^{+}$ ).

Fraction F2 exhibited the greatest potency to cause oxidative stress, so it was selected for further fractionation using reversed-phase, high-performance liquid chromatography (RP-HPLC). 50  $\mu$ L of F2 were injected, and fractionation was accomplished by use of a Betasil C18 column (5  $\mu$ m; 2.1 mm  $\times$  100 mm; Thermo Fisher Scientific). Ultrapure water (A) and methanol (B) were used as mobile phases. Initially, 5% B was increased to 30% over 5 min, then increased to 100% at 20 min and held static for 8 min, followed by a decrease to initial conditions of 5% B and held for 2.5 min to allow for column re-equilibration. The flow rate was 0.3 mL/min. The column and sample chamber temperatures were maintained at 30 and 10  $^{\circ}$ C, respectively. Fractions were collected at 0.5 min intervals obtaining a total of 60 subfractions.

**Nrf2 Bioassay.** The Nrf2 Luciferase reporter cell line (Signosis, Santa Clara, CA) was stably transfected with the pTA-NRF2-luciferase reporter vector. The amount of luciferase produced is directly proportional to the activation of Nrf2 signaling, and thus also proportional to the amount of oxidative stress present. The culture medium was Dulbecco's Modified Medium (DMEM) (Sigma, St. Louis, MO) supplemented with 10% (v/v) of fetal bovine serum (FBS) (Gibco, Grand Island, NY) and 75 mg/L of G418 (Life Technologies, Burlington, ON, Canada). The amount of FBS was reduced to 0.1% (v/v) in exposure media. Cells were incubated at 37  $^{\circ}$ C, in a 5% humidified CO<sub>2</sub> incubator. Fourth generation Nrf2 cells were used for assessing potency of extracts to activate Nrf2. Cells were seeded to 96-well flat bottom microplates with  $5 \times 10^4$  in 100  $\mu$ L per well, and were dosed after incubation overnight in exposure medium. A 5-fold dilution of TE or each fraction starting from 5 $\times$  was added to exposure medium to yield a final concentration of solvent of 0.1% (v/v). Cells were dosed with

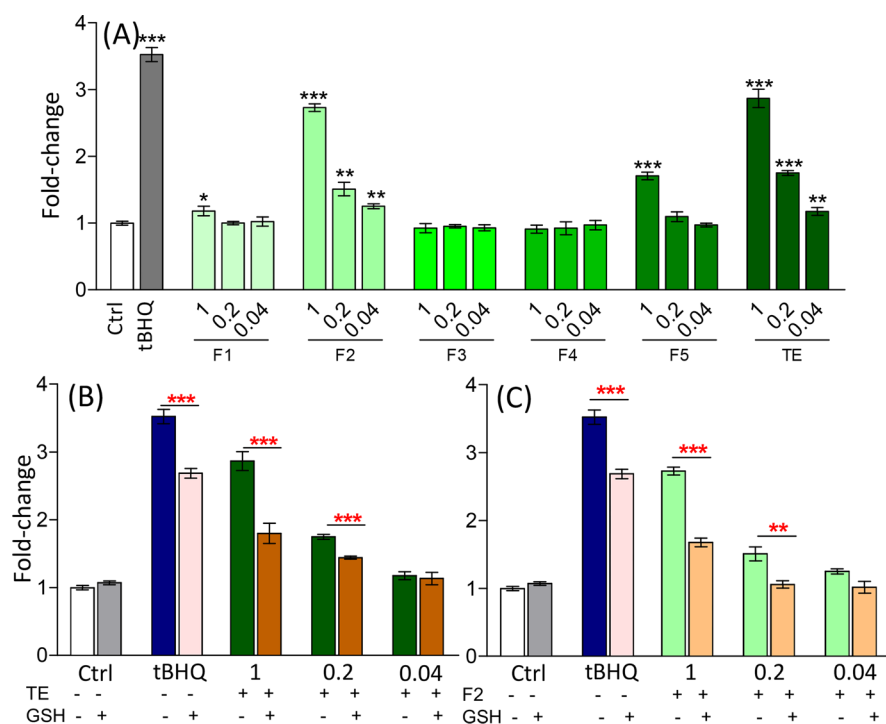


**Figure 1.** Effects of samples of OSPW on activity of Nrf2 cells. (A) Effects of the total extract (TE) and the five SPE fractions (F1–F5) of OSPW. (B) Effects of coexposure to 10 mmol/L of reduced GSH and the TE of OSPW. (C) Effects coexposure to 10 mmol/L of reduced GSH and F2. Averages of fold changes relative to a solvent control are given. Error bars represent standard deviation. Significance changes are indicated by an asterisk, where \*\*\* means  $p < 0.001$ , \*\* means  $p < 0.01$ , and \* means  $p < 0.05$ .

0.1% (v/v) of ethanol as the solvent control. Cells were exposed to the 60 subfractions of F2 at 1X without serial dilution because responses of Nrf2 were relatively small and the dose–response was linear. To confirm oxidative stress responses of exposed cells, rescue experiments were conducted by coexposing cells to 10 mM of reduced glutathione (GSH) (Sigma) with different concentrations of active fractions. Each concentration of each sample was conducted with four replicates. Cells were exposed to tBHQ (*tert*-butylhydroquinone, Sigma), which is a reference chemical known to activate Nrf2 through two-electron oxidation to form an electrophilic quinone in cells,<sup>26,28</sup> with 3-fold serial concentrations ranging from 50 to 0.6  $\mu$ M. Exposure of 5.6  $\mu$ M tBHQ was used as positive control in each plate. Response of Nrf2 cells to hydrogen peroxide ( $H_2O_2$ , Sigma), a well-known reactive oxidant, was also conducted (10 mM – 13.7  $\mu$ M, with 3-fold dilutions). After 16 h of exposure, activity of luciferase was detected by measurement of light produced by use of the SteadyLitePlus Kit (PerkinElmer, MA).

Cytotoxicity of fractions was measured by use of the 3-(4,5-dimethylthiazol-2-yl)-2,5-diphenyltetrazolium bromide (MTT) assay (Biotium, Hayward, CA). Cells were plated and exposed the same as in measurements of potency. An aliquot of 10  $\mu$ L of MTT was added per well and incubated for 4 h at 37  $^{\circ}$ C. Afterward, 200  $\mu$ L of DMSO was added to each well for 30 min to dissolve crystals of formazan. The  $OD_{570}$  of the supernatant was measured and corrected for background absorbance at 690 nm using a POLARStar OPTIMA microplate reader (BMG Labtech, Offenburg, Germany). If viability of cells was <80% of the solvent control, the corresponding exposure dose was considered as cytotoxic and therefore was not used in other exposures. No cytotoxicity occurred when Nrf2 cells were

exposed to 50  $\mu$ M or less of tBHQ, 1.1 mM or less of  $H_2O_2$ , or 1X or less of TE and fractions.

**Animal Care and Exposure of Medaka Embryos.** All work with fish was conducted according to the University of Saskatchewan’s Council on Animal Care and Supply (Protocol 20090108). Japanese medaka (*Oryzias latipes*) were cultured in the Aquatic Toxicology Research Facility at the University of Saskatchewan. Eggs were collected daily and maintained in embryo rearing medium (1 g/L NaCl, 0.030 g/L KCl, 0.040 g/L  $CaCl_2 \cdot H_2O$ , 80 mg/L  $MgSO_4$  and 1 mg/L Methylene Blue in distilled water) until hatch. All culturing of adult fish and rearing of embryos was conducted at a water temperature of 28  $^{\circ}$ C with a photoperiod of 16 h: 8 h (light: dark). Embryos at the fry stage of development (one-day posthatch,  $7 \pm 1$  dpf), which is the developmental stage that extends from hatching until appearance of fin rays in the caudal and pectoral fins<sup>29</sup> were collected immediately upon hatching. Twenty embryos were put into one Petri-dish, and were exposed to 0.1% of ethanol (negative control) or fractions of OSPW (F1–F5) at 0.5X or 0.25X of original concentration. Each exposure was conducted with three replicates ( $n = 3$ ), and exposure time was 1 h.

**Peroxidation of Lipids.** Peroxidation of lipids (LPO) was quantified in embryos of Japanese medaka after exposure. The lipid hydroperoxide assay kit (Cayman Chemical, Ann Arbor, MI) was used for determination of peroxidation of lipids according to recommendations of the manufacturer. Wet masses (mg) of the 20 embryos per exposure were determined prior to extraction of lipids. Samples were homogenized on ice and lipids were extracted with 500  $\mu$ L of chloroform containing 1% Triton X-100. The amount of lipid peroxide (nmol) was quantified by absorbance at 500 nm on a VersaMax Microplate

reader (Molecular Devices, Sunnyvale, CA). Data were normalized by the wet mass of embryos.

**Profiling of OSPW.** Chemical profiles and elemental composition for chemical species containing oxygen, nitrogen and sulfur, in each of fractionated samples, were determined by use of a Q Exactive mass spectrometer (Thermo Fisher Scientific) equipped with a Dionex UltiMate 3000 ultrahigh-performance liquid chromatography (UHPLC). Data was acquired in all ion fragment (AIF) mode. Parameters for AIF were, one full MS<sup>1</sup> scan (100–1,000 *m/z*) recorded at resolution *R* = 70 000 (at *m/z* 200) with a maximum of 3 × 10<sup>6</sup> ions collected within 100 ms, followed by one AIF MS/MS scan recorded at a resolution *R* = 35 000 (at *m/z* 200) with maximum of 1 × 10<sup>6</sup> ions collected within 60 ms. Details of this procedure are given in the SI.

**Data Analysis.** Linear regression of concentrations and fold changes than control was used to evaluate the bioanalytical equivalent concentrations of OSPW samples and H<sub>2</sub>O<sub>2</sub> for activation of Nrf2. The linear part of concentration–response relationships for activation of Nrf2 by tBHQ that was within 5-folds were used for linear regression.<sup>26</sup> The tBHQ equivalent factor (tBHQ-EF) of H<sub>2</sub>O<sub>2</sub> and tBHQ equivalent concentrations (tBHQ-EQ) of the TE and fractions of OSPW were calculated (eqs 1 and 2), based on concentrations that induced a response of 1.5-fold than control according to a previous study.<sup>26</sup>

$$t\text{BHQ} - \text{EF} = \frac{\text{Conc}_{t\text{BHQ}1.5}}{\text{Conc}_{\text{H}_2\text{O}_2 1.5}} \quad (1)$$

$$t\text{BHQ} - \text{EQ} = \frac{\text{Conc}_{t\text{BHQ}1.5}}{\text{Conc}_{\text{sample}1.5}} \quad (2)$$

where  $\text{Conc}_{t\text{BHQ}1.5}$ ,  $\text{Conc}_{\text{H}_2\text{O}_2 1.5}$ , and  $\text{Conc}_{\text{sample}1.5}$  are the calculated concentrations of tBHQ, TE or fractions, and H<sub>2</sub>O<sub>2</sub>, respectively, at which 1.5-fold of inductions relative to that of control were induced in Nrf2 cells.

Effects of treatments relative to controls and between treatments were evaluated by use of one-way ANOVA with Tukey's post hoc test. Differences were considered significant at a *p*-value < 0.05.

## RESULTS AND DISCUSSION

**Nrf2-mediated Oxidative Stress of OSPW.** A dose response was observed when Nrf2 cells were exposed to tBHQ (SI Figure S2), which is known to cause oxidative stress in vitro.<sup>26</sup> The maximal response was 20.3 ± 1.6 fold (*p* < 0.001) at a concentration of 16.7 μM of tBHQ. Considering the fact that oxidative stress may be caused by multiple oxidants and pathways, to test the method breadth, the Nrf2 system was also tested for another well-known reactive oxidant H<sub>2</sub>O<sub>2</sub>. Significant responses were induced by H<sub>2</sub>O<sub>2</sub> at concentrations of 13.7 to 1111.1 μM (SI Figure S2). According to the linear regression of H<sub>2</sub>O<sub>2</sub> concentrations and responses in Nrf2 cells (SI Figure S3), the tBHQ-EF of H<sub>2</sub>O<sub>2</sub> was determined to be 0.0063.

After benchmarking, the in vitro assay was applied to TE of OSPW. Activation of Nrf2 was significantly related to concentrations of TE (Figure 1A), while no cytotoxicity was observed at concentrations of 1× (or less) for TE. Maximal induction was 2.9 ± 0.14 fold (*p* < 0.001) at 1× of TE. A significant response was detected at 0.04× of the TE (1.2 ± 0.06 fold, *p* = 0.006), which was about 10-fold less than the

concentration of OSPW extracts (0.5×) that induced oxidative stress in primary cultures of rainbow trout hepatocytes,<sup>14</sup> which indicates the sensitivity of Nrf2 assay to oxidative stress caused by OSPW. However, differences in the source of OSPW, method of extraction, and unknowns regarding the profile of chemicals in the extract make direct comparison between these studies difficult. Regardless, multiple toxicities of OSPW have been reported, but with exception of activation of PPARγ signaling,<sup>21</sup> effects of OSPW at concentrations as small as those qualified here have not been reported.<sup>7,10,30</sup> According to the regression (SI Figure S3), the bioassay-derived tBHQ-EQ of TE was determined to be 7.06 μM. To further confirm that responses of Nrf2 to the TE were caused by generation of oxidative stress, coexposures of cells to TE and glutathione (GSH) were conducted. Reduced GSH is a well-known antioxidant preventing damage to important cellular components from reactive oxygen species. Exposure of 10 mM GSH did not influence the basal response of Nrf2 cells. The induction of Nrf2 cells by tBHQ was reduced to 76.3% (*p* < 0.001) by coexposure to 10 mM GSH (Figure 1B and C). When coexposed with 10 mM of reduced GSH, the response of Nrf2 to 1× or 0.2× of the TE were also significantly reduced to 62.8% (*p* < 0.001) and 82.4% (*p* < 0.001), respectively, of the response in cells exposed to the TE (Figure 1B). This result further confirmed that responses of Nrf2 to TE were mediated by oxidative stress.

### In Vitro and in Vivo Oxidative Stress of SPE Fractions.

To identify causative agents, the distribution of activations of Nrf2 among the five fractions that were generated by use of the SPE cartridges was determined. Three of the fractions (F1, F2 and F5) exhibited significant potency for activation of Nrf2, of which F2 was the most potent, with 2.7 ± 0.1 fold activation compared with that of the solvent control (*p* < 0.001). Activation of Nrf2 (1.1 ± 0.05, *p* = 0.021) was detected even at the least concentration of 0.04× of F2. Consistent with effects of the TE, when coexposed with GSH, activation of Nrf2 in cells exposed to 1× and 0.2× of F2 were significantly reduced to 61.5% (*p* < 0.001) and 79.7% (*p* = 0.01), respectively, (Figure 1C) of activation by exposure only to the fraction. Significant responses to F1 (1.2 ± 0.14 fold, *p* = 0.032) and F5 (1.7 ± 0.11 fold, *p* < 0.001) were observed, but only at the maximal concentration of 1× (Figure 1A). Because activity of Nrf2 was distributed among multiple SPE fractions, it suggested that multiple chemicals, with different polarities, in the aqueous phase of OSPW can cause oxidative stress. Based on predictions by use of linear regressions of concentration–response relationships for F1, F2, and F5 (SI Figure S2), the tBHQ-EQ of F1, F2, and F5 were 0.50 μM, 4.97 μM, and 1.92 μM, respectively. The summed tBHQ-EQ of these three fractions was 7.39 μM, which was similar to that of the TE (7.06 μM). This result indicated additive agonistic activities of multiple causative chemicals in fractions of OSPW, a result that was consistent with previous results for pure standards.<sup>26</sup>

Potencies of the five fractions to cause oxidative stress were further investigated in vivo by exposing freshly hatched embryos of Japanese medaka to 0.5× and 0.25× of each fraction, and quantifying hydroperoxidation of lipids (LPO) (Figure 2). This end point has been widely used as an in vivo biomarker of oxidative stress.<sup>7</sup> Significant production of LPO was detected (1.70 ± 0.26 fold, *p* < 0.001) only in embryos exposed to F2 at 0.5× of the original OSPW. Increased production of LPO was observed (1.40 ± 0.27 fold, *p* = 0.07), although not significant, in embryos exposed to F5 at 0.5× of

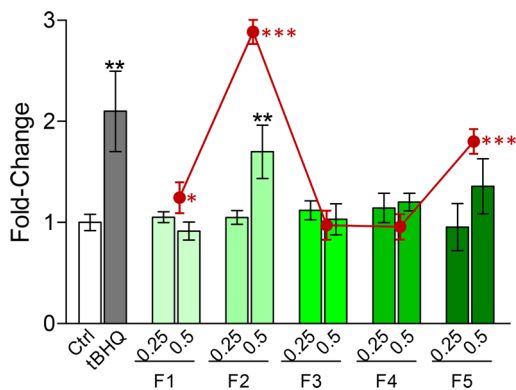


**Figure 2.** Fold changes of concentrations of lipid hydroperoxides (LPO) in embryos of Japanese medaka (1 day posthatch) after exposure to fractions of OSPW. Four replicates were conducted for each group ( $n = 4$ ), with 20 embryos in each replicate. Dots and line indicate fold changes induced in Nrf2 cells by F1–F5 at 1× of exposure. Significance is indicated by an asterisk, where \*\*\* means  $p < 0.001$ , \*\* means  $p < 0.01$ , and \* means  $p < 0.05$ .

the original OSPW. Oxidative stress responses to oil sands derived materials at the level of gene expression have also been reported for the nonbiting midge, *Chironomus dilutus*,<sup>31</sup> and fathead minnows exposed to OSPW<sup>7,9</sup> and embryos of Japanese medaka exposed to diluted bitumen.<sup>32</sup> The greater concentrations of reactive oxygen species in fathead minnows<sup>7</sup> and LPO in *Chironomus dilutus*<sup>31</sup> in other studies are consistent with results of this study, indicating that exposure of OSPW could cause oxidative stress. Greater in vivo oxidative stress caused by F2 and F5 was consistent with potencies for activation of Nrf2 observed in vitro for these fractions (as shown by red dots in Figure 2), which further supports use of the Nrf2 system for assessing oxidative stress caused by OSPW.

**Chemical Profiling of SPE Fractions.** A statistical strategy combined with untargeted chemical analysis was applied to identify specific chemicals in F2 that caused oxidative stress. A total of 16,037 peaks were detected across the five SPE fractions (Figure 3A). Among these, 3352 peaks were detected in ESI<sup>-</sup> and 12 685 peaks were detected in ESI<sup>+</sup>. While previous studies have focused on oxidative chemicals in OSPW detected

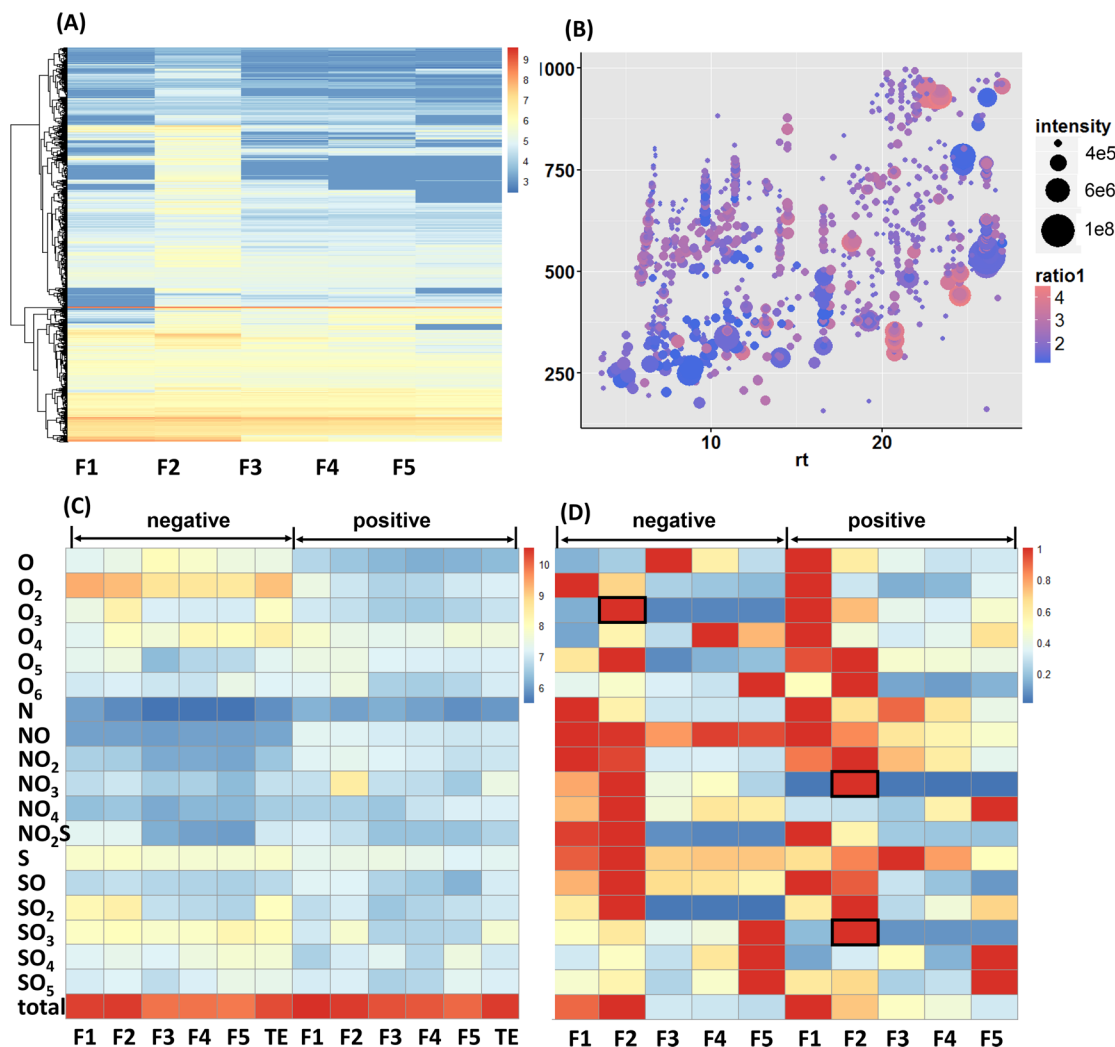


**Figure 3.** Distribution of species across SPE fractions. (A) Heatmap of peak abundances of all 16 037 detected peaks across five fractions. (B) Species exhibiting greater peak abundances in F2. The color is proportional to the log-transformed ratio of chemical abundances in F2 to those in F1. Sizes of dots are proportional to peak abundances of chemicals. (C) Heatmap of peak abundances of species from different fractions of SPE cartridges in both ESI<sup>-</sup> and ESI<sup>+</sup>. (D) Heatmap of species from different fractions of SPE cartridges after normalization to the maximal intensity. Black bordered areas indicate  $O_3^-$ ,  $NO_3^+$ , and  $SO_3^+$  species of chemicals that were associated with oxidative stress in F2.

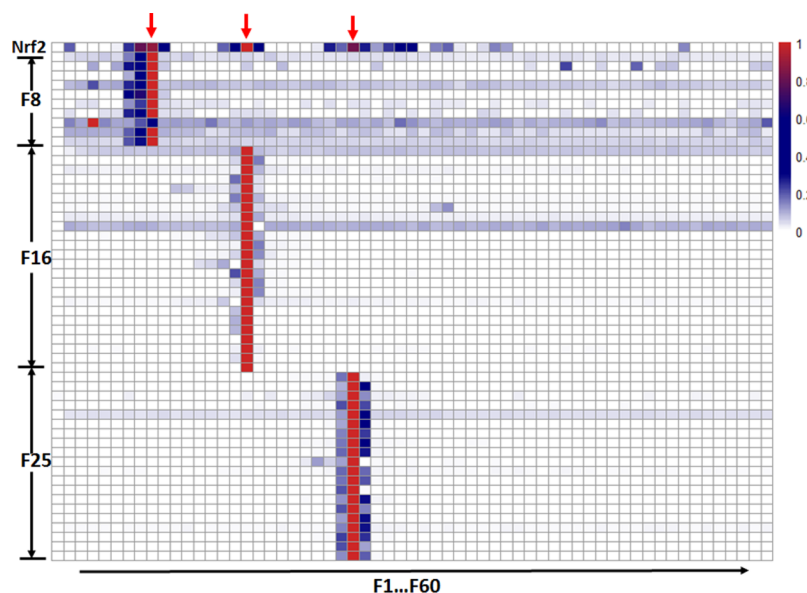


**Figure 4.** Distribution of Nrf2 activities and 54 proposed potential causative chemicals across 60 HPLC fractions of F2. The abundance of the activity and chemicals was normalized according to the maximal abundance in the 60 fractions. Red arrows indicated three bioactive fractions with Nrf2 activity detected. The first row indicated Nrf2 activity. Other rows indicated the normalized abundances of proposed causative chemicals identified in each group (F8, F16, F25).

by ESI<sup>-</sup>,<sup>13</sup> results of this study indicated 4-fold more chemicals could be detected in ESI<sup>+</sup>. Thus, if ESI<sup>-</sup> alone was applied for analysis, 60–80% of organic chemical constituents would not have been included in the analysis, thus limiting any conclusions regarding causative chemicals in the aqueous phase of OSPW.

While the total abundance of organic chemicals detected by use of both ESI<sup>-</sup> and ESI<sup>+</sup> was greater in F1 and F2 (Figure 3C), different chemical species exhibited distinct patterns of distribution among the five fractions. O<sup>+</sup> species and classic NAs (O<sub>2</sub><sup>-</sup> species) exhibited the greatest abundances in F1, while abundances of O<sub>3</sub><sup>-</sup>, O<sub>5</sub><sup>-</sup>, NO<sub>3</sub><sup>-</sup>, NO<sub>4</sub><sup>-</sup>, SO<sub>2</sub><sup>-</sup>, O<sub>6</sub><sup>+</sup>, NO<sub>3</sub><sup>+</sup>, SO<sub>2</sub><sup>+</sup>, and SO<sub>3</sub><sup>+</sup> species were greatest in F2 (Figure 3D). Because the greatest activation of Nrf2 and the greatest induction of LPO were observed in cells or in Japanese medaka exposed to F2, chemicals abundant in F2 were likely the causes of oxidative stress effects, but not classic NAs and O species that were most abundant in F1 (Figures 3C and D). Based on the strategy used for identification of causative chemicals, chemicals in F2 with total abundances 9.0-fold greater than those in F1 and 34-fold greater than those in F3 (see method details in SI) were considered as potential causative chemicals for induction of oxidative stress. Thus, potential causative chemicals in F2 were narrowed to 917 detected by use of ESI<sup>+</sup> and 162 detected by use of ESI<sup>-</sup>. Many of the individual chemicals were O<sub>3</sub><sup>-</sup>, NO<sub>3</sub><sup>+</sup>, and SO<sub>3</sub><sup>+</sup> species. These results indicated that the initial SPE fractionation removed more than 93% of chemicals from consideration as potential causative chemicals. The 1079 proposed potential causative chemicals exhibited variation in abundances of their peaks ( $2.1 \times 10^4$ – $1.4 \times 10^8$ ), retention times (3.6–27.0 min) and  $m/z$  values (156.3525–996.5622) (Figure 3B). According to their exact  $m/z$  values, formulas of several of the most abundant chemicals were predicted to be C<sub>30</sub>H<sub>62</sub>O<sub>4</sub>NS (rt = 26.1 min,  $m/z$  = 532.4404, abundance =  $6.2 \times 10^7$ ); C<sub>16</sub>H<sub>23</sub>O<sub>3</sub> (rt = 9.3 min,  $m/z$  = 263.1653, abundance =  $3.5 \times 10^7$ ); C<sub>15</sub>H<sub>21</sub>O<sub>3</sub> (rt = 7.8 min,  $m/z$  = 532.4404, intensity =  $6.2 \times 10^7$ ); C<sub>22</sub>H<sub>34</sub>O<sub>3</sub>S (rt = 19.2

min,  $m/z$  = 378.2219, intensity =  $2.3 \times 10^7$ ). Such results indicated that heteroatomic and polyoxygenated chemicals were specifically accumulated in F2. A Kendrick plot of the 1,079 chemicals further confirmed relatively great mass defects of these chemicals (SI Figure S4). Previous studies have reported that classic NAs (O<sub>2</sub><sup>-</sup>) often exhibit lesser mass defects (<0.1), whereas heteroatomic or polyoxygenated chemicals exhibit greater mass defects.<sup>33</sup> Results of this study indicated that heteroatomic and polyoxygenated chemicals, rather than classic NAs that were eluted in F1, are potential causative chemicals of oxidative stress in aquatic organisms exposed to OSPW.

Only small amounts of organic chemicals were detected in F5 (methanol fraction) (Figure 3C), even though this fraction exhibited relatively great potency for activation of Nrf2. Such results indicated that some specific, highly polar chemicals could be responsible for the potency observed in that fraction. Several species containing greater numbers of oxygen atoms (O<sub>6</sub><sup>-</sup>, SO<sub>3</sub><sup>-</sup>, SO<sub>4</sub><sup>-</sup>, SO<sub>5</sub><sup>-</sup>, NO<sub>4</sub><sup>+</sup>, SO<sub>4</sub><sup>+</sup>, and SO<sub>5</sub><sup>+</sup>) were specifically enriched in F5. Enrichment of these chemicals in F5 can be attributed to the greater numbers of oxygen and concomitantly greater polarities, which could be eluted from SPE cartridges by more polar solvent, methanol. The greater contents of oxygen in these chemicals might also contribute to their reactive oxidative activity. Results of previous studies have demonstrated that chemicals with greater oxygen (phenol, ketone), such as tBHQ, often caused oxidative stress.<sup>34</sup> Recently, it was reported that the SO<sub>3</sub><sup>-</sup> species in OSPW were responsible for cytotoxicity of yeast through oxidative stress and detrimental effects on cellular membranes,<sup>13</sup> which is consistent with the specific accumulation of SO<sub>3</sub><sup>-</sup> species in F5 observed in the present study. However, that study focused on detoxification of OSPW by algae.<sup>13</sup> Our results showed that many other chemicals in OSPW may also contribute to oxidative stress. Although a potential limitation of the present study is that some chemical species may be lost during the SPE pretreatment step, most chemical species showed sufficient

Table 1. 10 Most Abundant Species Proposed to Cause Nrf2 Activity Identified by Effect Directed Assay

fraction # <sup>a</sup>	m/z	rt (min) <sup>c</sup>	intensity <sup>b</sup>	ion mode	formula <sup>e</sup>	mass error <sup>d</sup>
F2.25	327.1991	12.7	6.1e6	ESI <sup>+</sup>	C <sub>18</sub> H <sub>31</sub> O <sub>3</sub> S	0.79
F2.25	341.2147	12.6	4.5e6	ESI <sup>+</sup>	C <sub>19</sub> H <sub>33</sub> O <sub>3</sub> S	0.61
F2.25	353.2146	12.6	3.5e6	ESI <sup>+</sup>	C <sub>20</sub> H <sub>34</sub> O <sub>3</sub> S	0.31
F2.16	212.0745	7.82	3.0e6	ESI <sup>+</sup>	C <sub>10</sub> H <sub>14</sub> O <sub>2</sub> NS	2.5
F2.25	361.1817	12.6	2.6e6	ESI <sup>+</sup>	C <sub>19</sub> H <sub>27</sub> O <sub>2</sub> N <sub>3</sub> S	-0.41
F2.25	329.2146	12.6	2.5e6	ESI <sup>+</sup>	C <sub>18</sub> H <sub>33</sub> O <sub>3</sub> S	0.33
F2.25	355.2302	12.6	1.9e6	ESI <sup>+</sup>	C <sub>20</sub> H <sub>35</sub> O <sub>3</sub> S	0.44
F2.16	263.1643	8.06	1.7e6	ESI <sup>+</sup>	C <sub>16</sub> H <sub>23</sub> O <sub>3</sub>	0.49
F2.16	329.1751	8.18	1.6e6	ESI <sup>+</sup>	C <sub>20</sub> H <sub>25</sub> O <sub>4</sub>	-0.40
F2.25	320.2222	12.7	1.4e6	ESI <sup>+</sup>	C <sub>19</sub> H <sub>30</sub> O <sub>3</sub> N	0.56

<sup>a</sup>The subfraction number of the corresponding causative species. <sup>b</sup>The absolute peak intensity of causative specie peaks. <sup>c</sup>Predicted formulas for [M + H]<sup>+</sup> based on exact mass, isotopic peak and MS<sup>2</sup> information. <sup>d</sup>Mass error (ppm) of the predicted formulas. <sup>e</sup>Retention time.

recoveries, for example, the recovery of SO<sub>4</sub><sup>+</sup> specie was only 30.9%. Thus, further evaluation of oxidative stress response of OSPW extracted by different methods is warranted in future studies.

**Identification of Causative Chemicals by HPLC Fractionation.** Although SPE fractionation excluded 93% of inactive chemicals, 1,079 potential causative chemicals were still present in F2, which was the most potent fraction for activation of Nrf2 and was the only fraction that caused significant induction of LPO. To decrease the number of false identifications, HPLC fractionation of F2 was further conducted to identify potential causative chemicals. Among the 60 subfractions, activation of Nrf2 was identified in three primary groups centered on fraction F2.8 (1.30-fold, *p* < 0.001), F2.16 (1.34-fold, *p* < 0.001) and F2.25 (1.28-fold, *p* < 0.001) (Figure 4). Thus, in F2, at least three groups of chemicals could be responsible for the activation of Nrf2. Similar to the SPE fractions, the summed activity in these three fractions was 2.2-fold, which was slightly less than that in F2 (2.7-fold), supporting the possibility of additive effects in these fractions, and the preservation of most bioactive chemicals during HPLC fractionation.

Chemicals in active subfractions were identified by use of an untargeted chemical analysis strategy involving three steps (SI Figure S5). First, chemicals in subfractions that exhibited potency for activation of Nrf2 were identified, then these chemical peaks were matched across different fractions. Second, the interferences from these subfractions were excluded according to the statistical strategy and the activity pattern (see Method section in SI) among these subfractions (e.g., 15 chemicals were specifically enriched in F2.8). Third, only chemicals identified as potential causative chemicals from the SPE step were proposed as potential causative chemicals in the subfraction of F2 (e.g., 10 chemicals were finally identified in F2.8). Based on this three-step workflow, only 10, 24, and 20 chemicals were proposed as potential causative chemicals in F2.8, F2.16, and F2.25, respectively. Predicted formulas, and exact mass information for 10 of the most abundant causative chemicals were presented (Table 1). Consistent with results of the SPE fractionation, heteroatomic chemicals (e.g., SO<sub>3</sub><sup>+</sup>) and/or chemicals with great number of oxygen (e.g., O<sub>4</sub><sup>+</sup>) were proposed as the putative causative chemicals. Several analogues, with different double bond equivalency or carbon number were identified (i.e., C<sub>18</sub>H<sub>31</sub>SO<sub>3</sub> and C<sub>19</sub>H<sub>33</sub>SO<sub>3</sub>) (Table 1).

Relatively great abundances of several SO<sub>3</sub><sup>+</sup> and O<sub>3</sub><sup>+</sup> chemicals enabled collection of ultrahigh-resolution MS<sup>2</sup> spectra of these chemicals, from which potential structures

for formulas predicted from accurate masses could be proposed. Interferences of the MS<sup>2</sup> were further excluded by correlating all ions in the spectra with those of precursor ions. Ions that exhibited poor correlations were discarded, as described previously.<sup>21</sup> Based on this strategy, “clean” MS<sup>2</sup> spectra of fragmentation patterns were obtained for an abundant SO<sub>3</sub><sup>+</sup> chemical (predicted formula was C<sub>18</sub>H<sub>31</sub>O<sub>3</sub>S) and O<sub>3</sub><sup>+</sup> chemical (predicted formula was C<sub>16</sub>H<sub>23</sub>O<sub>3</sub>). Stepwise neutral loss of two H<sub>2</sub>O, and one CO group clearly indicated that two hydroxyl groups and one aldehyde group were contained in the O<sub>3</sub><sup>+</sup> chemical (Figure 5A). Patterns of fragmentations of SO<sub>3</sub><sup>+</sup> chemicals are similar to those of O<sub>3</sub><sup>+</sup> chemicals. Neutral loss of H<sub>2</sub>O and CO group was also clearly observed (Figure 5B). The lack of SH fragments indicated that thiol groups were not contained in the SO<sub>3</sub><sup>+</sup> chemical, and the sulfur atom was contained as an inserted chain. Such results indicated that hydroxylated aldehydes are major oxidative chemicals in

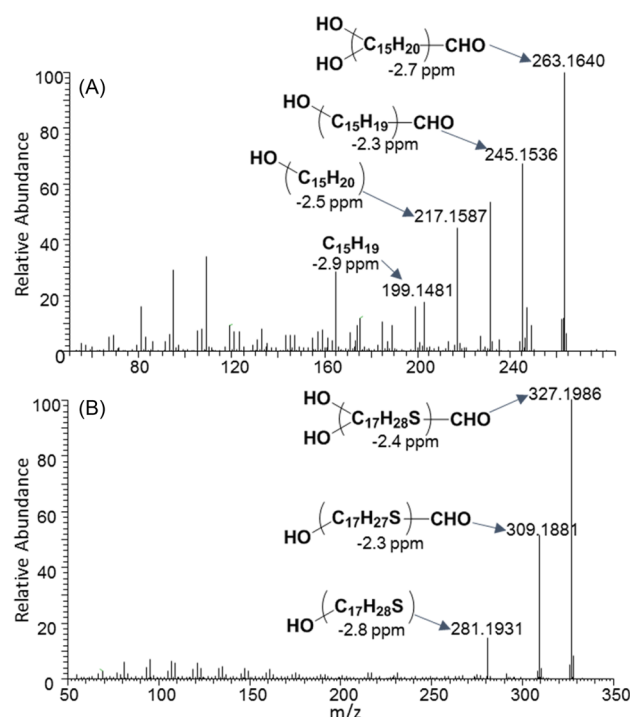


**Figure 5.** High resolution MS<sup>2</sup> and predicted chemical structures of O<sub>3</sub><sup>+</sup> (top, formula was predicted as C<sub>16</sub>H<sub>22</sub>O<sub>3</sub>) and SO<sub>3</sub><sup>+</sup> (bottom, formula was predicted as C<sub>18</sub>H<sub>30</sub>SO<sub>3</sub>) species identified as causing oxidative stress.

OSPW. Previous studies have reported that hydroxylated aldehydes could be potent inducers of oxidative stress by covalently binding to cysteine residues of protein, which was consistent with basic principle of disruption of the Keap1-Nrf2 complex.<sup>35</sup> Further studies are warranted in which these O<sub>3</sub><sup>+</sup> and SO<sub>3</sub><sup>+</sup> species are synthesized and used to determine concentrations in OSPW and to confirm their role in oxidative stress.

**Implications.** Systematic evaluation of toxic effects of OSPW and identification of toxic components is needed to specify priority chemicals or toxicities that could be monitored to assess potential environmental effects and detoxification of OSPW stored in EPLs. However, this is a great challenge because of the complexity of chemical constituents in OSPW. By combining a reproducible in vitro assay, a powerful statistical strategy and untargeted chemical analysis, this study, for the first time, successfully narrowed the number of chemicals responsible for induction of oxidative stress by OSPW from ~16 000 to 54. Polyoxygenated chemicals, especially hydroxylated aldehyde chemicals, rather than classically defined NAs, were the primary chemicals in the aqueous phase of OSPW that caused oxidative stress. In contrast to traditional EDA, inclusion of semiquantitative dose–response information and untargeted chemical analysis allowed unbiased, efficient focusing of the list of potential chemicals. Such a strategy could be used as a general approach for identification of other toxic chemicals in OSPW, including endocrine disruptive chemicals.

## ■ ASSOCIATED CONTENT

### 📄 Supporting Information

The Supporting Information is available free of charge on the ACS Publications website at DOI: [10.1021/acs.est.7b01987](https://doi.org/10.1021/acs.est.7b01987).

Text and figures addressing (1) Profiling of OSPW; (2) Fractionation strategy of OSPW; (3) Dose–response relationships of tBHQ and H<sub>2</sub>O<sub>2</sub> in Nrf2 cells; (4) Linear regressions of concentrations and responses in Nrf2 cells for tBHQ, H<sub>2</sub>O<sub>2</sub>, TE, F1, F2, F5; (5) Kendrick plot of potential causative chemicals; and (6) Three-step data analysis to identify causative chemicals in HPLC subfractions of F2 (PDF)

## ■ AUTHOR INFORMATION

### Corresponding Authors

\*(H.P.) Phone: +1-306-966-8733; fax: +1-306 966 4796; e-mail: [huisci@gmail.com](mailto:huisci@gmail.com).

\*(S.W.) Phone: +1-403-329-2320; e-mail: [steve.wiseman@uleth.ca](mailto:steve.wiseman@uleth.ca).

### ORCID

Hui Peng: [0000-0002-2777-0588](https://orcid.org/0000-0002-2777-0588)

### Notes

The authors declare no competing financial interest.

## ■ ACKNOWLEDGMENTS

This research was supported by a Collaborative Research and Development Grant from the Natural Science and Engineering Research Council of Canada and Syncrude Canada Ltd. to J.P. Giesy (Project # C4288) and, in part, by a Discovery Grant from the Natural Science and Engineering Research Council of Canada (Project # 326415–07) to J.P. Giesy, and a grant from the Western Economic Diversification Canada (Projects #

6578, 6807). The authors acknowledge the support of an instrumentation grant from the Canada Foundation for Innovation. S. Wiseman was supported by the Canada Research Chair program. J.P. Giesy was supported by the Canada Research Chair program, the 2014 “High Level Foreign Experts” (#GDT20143200016) program, funded by the State Administration of Foreign Experts Affairs, the P.R. China to Nanjing University, a Distinguished Visiting Professorship at the Department of Biology and Chemistry and State Key Laboratory in Marine Pollution, City University of Hong Kong, and the Einstein Professor Program of the Chinese Academy of Sciences. The authors thank Syncrude Canada Ltd. for supplying the OSPW.

## ■ REFERENCES

- (1) CAPP (Canadian Association of Petroleum Producers), Crude Oil Forecast, Markets and Pipeline Expansions. CAPP, June 2007.
- (2) CAPP, Crude oil forecast, markets & transportation. Canadian association of petroleum producers, Calgary, Alberta, p. 5. 2015.
- (3) Kelly, E. N.; Schindler, D. W.; Hodson, P. V.; Short, J. W.; Radmanovich, R.; Nielsen, C. C. Oil sands development contributes elements toxic at low concentrations to the Athabasca River and its tributaries. *Proc. Natl. Acad. Sci. U. S. A.* **2010**, *107* (37), 16178–16183.
- (4) Ross, M. S.; Pereira, A. d. S.; Fennell, J.; Davies, M.; Johnson, J.; Sliva, L.; Martin, J. W. Quantitative and qualitative analysis of naphthenic acids in natural waters surrounding the Canadian oil sands industry. *Environ. Sci. Technol.* **2012**, *46* (23), 12796–12805.
- (5) Gosselin, P.; Hruday, S. E.; Naeth, M. A.; Plourde, A.; Therrien, R.; Van Der Kraak, G.; Xu, Z. *Environmental and Health Impacts of Canada's Oil Sands Industry*; Royal Society of Canada Expert panel report: Ottawa, ON, 2010.
- (6) Morandi, G. D.; Wiseman, S.; Pereira, A. D. S.; Mankidy, R.; Gault, I. G.; Martin, J. W.; Giesy, J. P. Effects-Directed Analysis of Dissolved Organic Compounds in Oil Sands Process Affected Water (OSPW). *Environ. Sci. Technol.* **2015**, *49*, 12395.
- (7) He, Y.; Patterson, S.; Wang, N.; Hecker, M.; Martin, J. W.; El-Din, M. G.; Giesy, J. P.; Wiseman, S. B. Toxicity of untreated and ozone-treated oil sands process-affected water (OSPW) to early life stages of the fathead minnow (*Pimephales promelas*). *Water Res.* **2012**, *46* (19), 6359–6368.
- (8) Wu, B.; Liu, S.; Guo, X. C.; Zhang, Y.; Zhang, X. X.; Li, M.; Cheng, S. P. Responses of Mouse Liver to Dechlorane Plus Exposure by Integrative Transcriptomic and Metabonomic Studies. *Environ. Sci. Technol.* **2012**, *46* (19), 10758–10764.
- (9) Wiseman, S. B.; He, Y.; Gamal-El Din, M.; Martin, J. W.; Jones, P. D.; Hecker, M.; Giesy, J. P. Transcriptional responses of male fathead minnows exposed to oil sands process-affected water. *Comp. Biochem. Physiol., Part C: Toxicol. Pharmacol.* **2013**, *157* (2), 227–235.
- (10) He, Y.; Wiseman, S. B.; Wang, N.; Perez-Estrada, L. A.; El-Din, M. G.; Martin, J. W.; Giesy, J. P. Transcriptional responses of the brain–gonad–liver axis of fathead minnows exposed to untreated and ozone-treated oil sands process-affected water. *Environ. Sci. Technol.* **2012**, *46* (17), 9701–9708.
- (11) Kavanagh, R. J.; Frank, R. A.; Oakes, K. D.; Servos, M. R.; Young, R. F.; Fedorak, P. M.; MacKinnon, M. D.; Solomon, K. R.; Dixon, D. G.; Van Der Kraak, G. Fathead minnow (*Pimephales promelas*) reproduction is impaired in aged oil sands process-affected waters. *Aquat. Toxicol.* **2011**, *101* (1), 214–220.
- (12) Marentette, J. R.; Frank, R. A.; Bartlett, A. J.; Gillis, P. L.; Hewitt, L. M.; Peru, K. M.; Headley, J. V.; Brunswick, P.; Shang, D. Y.; Parrott, J. L. Toxicity of naphthenic acid fraction components extracted from fresh and aged oil sands process-affected waters, and commercial naphthenic acid mixtures, to fathead minnow (*Pimephales promelas*) embryos. *Aquat. Toxicol.* **2015**, *164*, 108–117.
- (13) Quesnel, D. M.; Oldenburg, T. B. P.; Larter, S. R.; Gieg, L. M.; Chua, G. Biostimulation of oil sands process-affected water with

phosphate yields removal of sulfur-containing organics and detoxification. *Environ. Sci. Technol.* **2015**, *49* (21), 13012–13020.

(14) Gagné, F.; Douville, M.; André, C.; Debenest, T.; Talbot, A.; Sherry, J.; Hewitt, L.; Frank, R.; McMaster, M.; Parrott, J. Differential changes in gene expression in rainbow trout hepatocytes exposed to extracts of oil sands process-affected water and the Athabasca River. *Comp. Biochem. Physiol., Part C: Toxicol. Pharmacol.* **2012**, *155* (4), 551–559.

(15) Headley, J. V.; McMartin, D. W. A review of the occurrence and fate of naphthenic acids in aquatic environments. *J. Environ. Sci. Health, Part A: Toxic/Hazard. Subst. Environ. Eng.* **2004**, *39* (8), 1989–2010.

(16) Pereira, A. S.; Bhattacharjee, S.; Martin, J. W. Characterization of oil sands process-affected waters by liquid chromatography orbitrap mass spectrometry. *Environ. Sci. Technol.* **2013**, *47* (10), 5504–5513.

(17) Headley, J. V.; Peru, K. M.; Fahlman, B.; Colodey, A.; McMartin, D. W. Selective solvent extraction and characterization of the acid extractable fraction of Athabasca oils sands process waters by Orbitrap mass spectrometry. *Int. J. Mass Spectrom.* **2013**, *345*, 104–108.

(18) Jones, D.; Scarlett, A. G.; West, C. E.; Frank, R. A.; Gieleciak, R.; Hager, D.; Pureveen, J.; Tegelaar, E.; Rowland, S. J. Elemental and spectroscopic characterization of fractions of an acidic extract of oil sands process water. *Chemosphere* **2013**, *93* (9), 1655–1664.

(19) MacKinnon, M.; Boerger, H. Description of Two Treatments for Detoxifying Oil Sands Tailings Pond Water. *Wat. Pollut. Res. J. Canada* **1986**, *21*, 496–512.

(20) Morandi, G. D.; Wiseman, S. B.; Pereira, A.; Mankidy, R.; Gault, I. G. M.; Martin, J. W.; Giesy, J. P. Effects-directed analysis of dissolved organic compounds in oil sands process-affected water. *Environ. Sci. Technol.* **2015**, *49* (20), 12395–12404.

(21) Peng, H.; Sun, J.; Alharbi, H. A.; Jones, P. D.; Giesy, J. P.; Wiseman, S. B. Peroxisome proliferator-activated receptor  $\gamma$  is a sensitive target for oil sands process-affected water: effects on adipogenesis and identification of ligands. *Environ. Sci. Technol.* **2016**, *50* (14), 7816–7824.

(22) Hecker, M.; Giesy, J. P., Effect-directed analysis of Ah-receptor mediated toxicants, mutagens, and endocrine disruptors in sediments and biota. In *Effect-Directed Analysis of Complex Environmental Contamination*; Springer: 2011; pp 285–313.

(23) Brack, W. Effect-directed analysis: a promising tool for the identification of organic toxicants in complex mixtures? *Anal. Bioanal. Chem.* **2003**, *377* (3), 397–407.

(24) Nguyen, T.; Nioi, P.; Pickett, C. B. The Nrf2-antioxidant response element signaling pathway and its activation by oxidative stress. *J. Biol. Chem.* **2009**, *284* (20), 13291–13295.

(25) Zhang, Q.; Pi, J.; Woods, C. G.; Andersen, M. E. A systems biology perspective on Nrf2-mediated antioxidant response. *Toxicol. Appl. Pharmacol.* **2010**, *244* (1), 84–97.

(26) Escher, B. I.; van Daele, C.; Dutt, M.; Tang, J. Y.; Altenburger, R. Most oxidative stress response in water samples comes from unknown chemicals: the need for effect-based water quality trigger values. *Environ. Sci. Technol.* **2013**, *47* (13), 7002–7011.

(27) Alharbi, H. A.; Saunders, D. M.; Al-Mousa, A.; Alcorn, J.; Pereira, A. S.; Martin, J. W.; Giesy, J. P.; Wiseman, S. B. Inhibition of ABC transport proteins by oil sands process affected water. *Aquat. Toxicol.* **2016**, *170*, 81–88.

(28) Wang, X. J.; Hayes, J. D.; Wolf, C. R. Generation of a stable antioxidant response element-driven reporter gene cell line and its use to show redox-dependent activation of Nrf2 by cancer chemotherapeutic agents. *Cancer Res.* **2006**, *66* (22), 10983–10994.

(29) Iwamatsu, T. Stages of normal development in the medaka *Oryzias latipes*. *Mech. Dev.* **2004**, *121* (7), 605–618.

(30) He, Y.; Wiseman, S. B.; Hecker, M.; Zhang, X.; Wang, N.; Perez, L. A.; Jones, P. D.; Gamal El-Din, M.; Martin, J. W.; Giesy, J. P. Effect of ozonation on the estrogenicity and androgenicity of oil sands process-affected water. *Environ. Sci. Technol.* **2011**, *45* (15), 6268–6274.

(31) Wiseman, S.; Anderson, J.; Liber, K.; Giesy, J. Endocrine disruption and oxidative stress in larvae of *Chironomus dilutus*

following short-term exposure to fresh or aged oil sands process-affected water. *Aquat. Toxicol.* **2013**, *142*, 414–421.

(32) Madison, B. N.; Hodson, P.; Langlois, V. Diluted bitumen causes deformities and molecular responses indicative of oxidative stress in Japanese medaka embryos. *Aquat. Toxicol.* **2015**, *165*, 222–230.

(33) Hughey, C. A.; Hendrickson, C. L.; Rodgers, R. P.; Marshall, A. G.; Qian, K. N. Kendrick mass defect spectrum: A compact visual analysis for ultrahigh-resolution broadband mass spectra. *Anal. Chem.* **2001**, *73* (19), 4676–4681.

(34) Imhoff, B. R.; Hansen, J. M. Tert-butylhydroquinone induces mitochondrial oxidative stress causing Nrf2 activation. *Cell Biol. Toxicol.* **2010**, *26* (6), 541–551.

(35) Grimsrud, P. A.; Xie, H.; Griffin, T. J.; Bernlohr, D. A. Oxidative stress and covalent modification of protein with bioactive aldehydes. *J. Biol. Chem.* **2008**, *283* (32), 21837–21841.

## Supporting Information

For

### Identification of Chemicals that Cause Oxidative Stress in Oil Sands Process-Affected Water

Jianxian Sun<sup>a</sup>, Hui Peng<sup>\*a</sup>, Hattan A. Alharbi<sup>a</sup>, Paul D. Jones<sup>a,b</sup>, John. P. Giesy<sup>a,b,c,d,e,f,g</sup>, and Steve B. Wiseman<sup>\*h</sup>

<sup>a</sup>Toxicology Centre, University of Saskatchewan, 44 Campus Drive, Saskatoon, SK, Canada

<sup>b</sup>School of Environment and Sustainability, 117 Science Place, Saskatoon, SK, Canada

<sup>c</sup>Department of Veterinary Biomedical Sciences, University of Saskatchewan, Saskatoon, SK, Canada

<sup>d</sup>Zoology Department, Center for Integrative Toxicology, Michigan State University, East Lansing, MI, USA

<sup>e</sup>School of Biological Sciences, University of Hong Kong, Hong Kong Special Administrative Region, Peoples republic of China

<sup>f</sup>State Key Laboratory of Pollution Control and Resource Reuse, School of the Environment, Nanjing University, Nanjing, People's Republic of China

<sup>g</sup>Biology Department, Hong Kong Baptist University, Hong Kong, SAR, China

<sup>h</sup>Department of Biological Sciences, University of Lethbridge, Lethbridge, Alberta T1K 3M4, Canada

**\*Corresponding author: Hui Peng, [huisci@gmail.com](mailto:huisci@gmail.com), Toxicology Centre, University of Saskatchewan, Saskatoon, SK, Canada; Tel.: +1-306-966-8733; Fax: +1-306 966 4796; Steve Wiseman, [steve.wiseman@uleth.ca](mailto:steve.wiseman@uleth.ca), Department of Biological Sciences, University of Lethbridge, Lethbridge, AB, Canada; Tel.: +1-403-329-2320**

Words 505

Figures 5

Tables 0

This supporting information provides text and figures addressing (1) Chemical profiling of OSPW; (2) Fractionation strategy of OSPW; (3) Dose-response relationships of tBHQ and H<sub>2</sub>O<sub>2</sub> in Nrf2 cells; (4) Linear regressions of concentrations and responses in Nrf2 cells; (5) Kendrick plot of potential causative chemicals; and (6) Three-step data analysis strategy to identify causative chemicals in HPLC sub-fractions.

**Chemical profiling of OSPW.** Aliquots of extracts were analyzed using a Q Exactive UHRMS (Thermo Fisher Scientific) equipped with a Dionex™ UltiMate 3000 UHPLC system (Thermo Fisher Scientific). Separation of chemicals was achieved by use of a Betasil C18 column (5  $\mu$ m; 2.1 mm  $\times$  100 mm; Thermo Fisher Scientific). Injection volume was 5  $\mu$ L. Ultrapure water (A) and methanol (B) were used as mobile phases. Initially 5% B was increased to 60% in 7 min, then increased to 100% at 20 min and held static for 10 min, followed by a decrease to initial conditions of 5% B and held for 3 min to allow for equilibration. Rate of flow was 0.40 mL/min. The column and sample compartment temperatures were maintained at 30 °C and 10 °C, respectively. Data was acquired in all ion fragment (AIF) mode. Parameters for AIF were, one full MS<sup>1</sup> scan (100-1,000  $m/z$ ) recorded at resolution R=70,000 (at  $m/z$  200) with a maximum of  $3 \times 10^6$  ions collected within 100 ms, followed by one AIF MS/MS scan recorded at a resolution R=35,000 (at  $m/z$  200) with maximum of  $1 \times 10^6$  ions collected within 60 ms. The general mass spectrometry settings for electrospray ionization (ESI) mode were as follows: spray voltage, 2.8 kV; capillary temperature, 350 °C; sheath Gas, 35 L/h; auxiliary gas, 8 L/h; probe heater temperature, 350 °C.

Untargeted mass spectrometry data analysis was accomplished with an in-house R version 3.1.2 (R Foundation for Statistical Computing, Vienna, Austria). Raw mass spectrometry files were converted to mzXML format. The mass spectrometry data and initial peaks were detected with XCMS package which has been used widely for metabolomics studies.<sup>1</sup> After adjustment of retention time, peaks among different samples were matched and grouped together. Causative chemicals were first identified from peaks in F2 according to

the potency folds of F2 in Nrf2 cells compared with F1 and F3. The tBHQ-EQ of F2 in Nrf2 cells was 4.5  $\mu$ M, which was 9.0-fold greater than that in F1 (0.5  $\mu$ M), and 34-fold greater than that in F3 (<0.13  $\mu$ M).

$$F_2 / F_3 = \frac{\text{response}_{F_2} - 1}{\text{response}_{F_3} - 1} \quad (\text{S1})$$

Where  $\text{response}_{F_2}$  and  $\text{response}_{F_3}$  are fold changes of responses in Nrf2 cells induced by F2 and F3. Since Nrf2 cells did not show any response after exposure to F3, a background of 1.05 fold (tBHQ-EQ was 0.13  $\mu$ M) was used for the calculation.

Using this strategy, only peaks exhibiting 9.0-fold greater peak intensities in F2 than in F1, and 34-fold greater than F3 were considered as potentially causative chemicals for activation of Nrf2. To confirm these results the final differentiated peak list from output of the R program was checked manually by use of exact  $MS^1$  masses and retention times. Elemental compositions of causative chemicals were calculated using an in-house R program, in which the mass tolerance was set to 5 ppm. Chemical formulas were set to contain up to 100C, 200 H, 8 N, 10 O, and 5 S per molecule.<sup>2</sup> Considering the potential existence of multiple adducts for a given ion, neutral compound formula was not calculated and formulas of ions were provided instead.

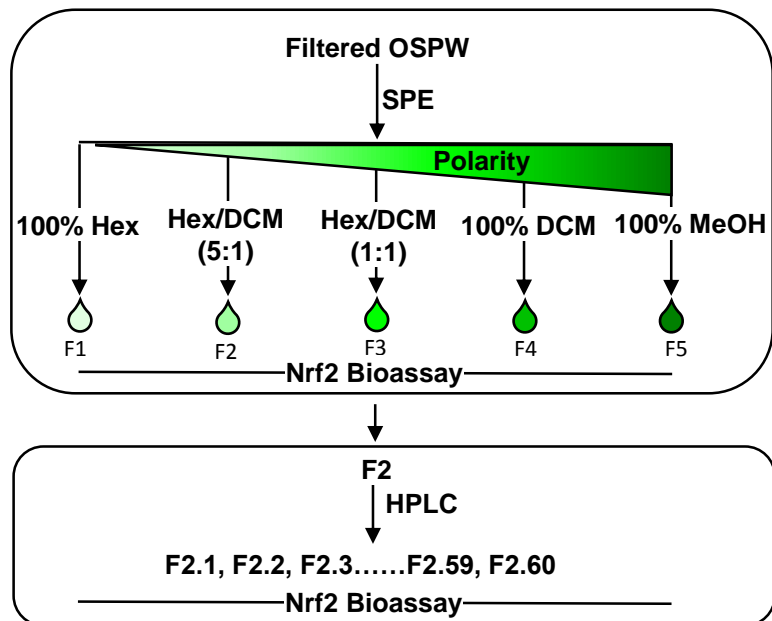


**Figure S1.** Fractionation strategy of oil sands process-affected water. Fractions from SPE were eluted with 6 mL solvents in sequence from left to right, and active fraction (F2) was selected for further HPLC fractionation.

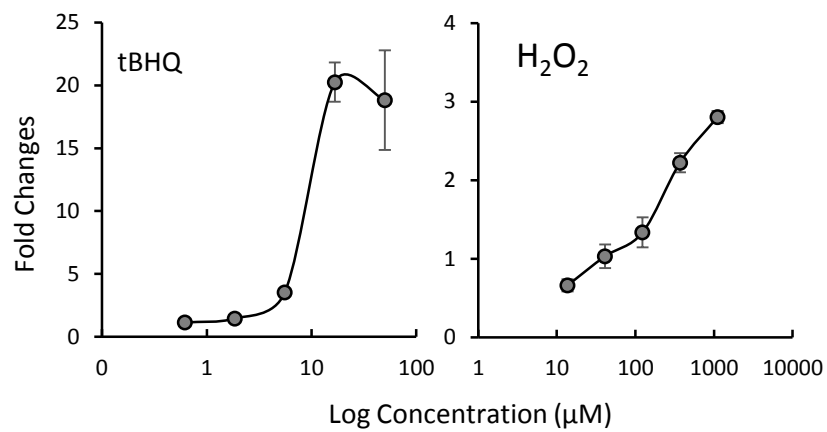


**Figure S2.** Dose-response relationships activation of Nrf2 signaling and concentrations of tBHQ and H<sub>2</sub>O<sub>2</sub>.

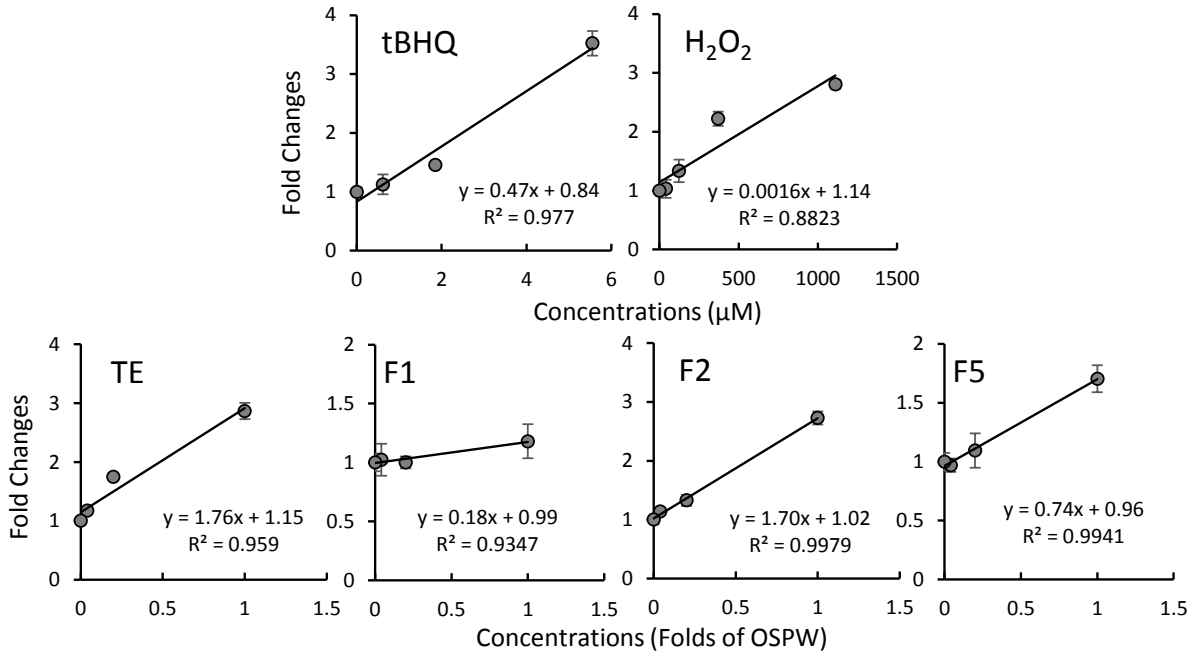


**Figure S3.** Linear regressions of concentrations and responses in Nrf2 cells for tBHQ ( $p = 0.012$ ), H<sub>2</sub>O<sub>2</sub> ( $p = 0.018$ ), the TE of OSPW ( $p = 0.021$ ), and OSPW fractions F1 ( $p = 0.033$ ), F2 ( $p = 0.001$ ), and F5 ( $p = 0.003$ ). The linear part of concentration-response relationships within 5 folds of induction compared to control were used for linear regression.

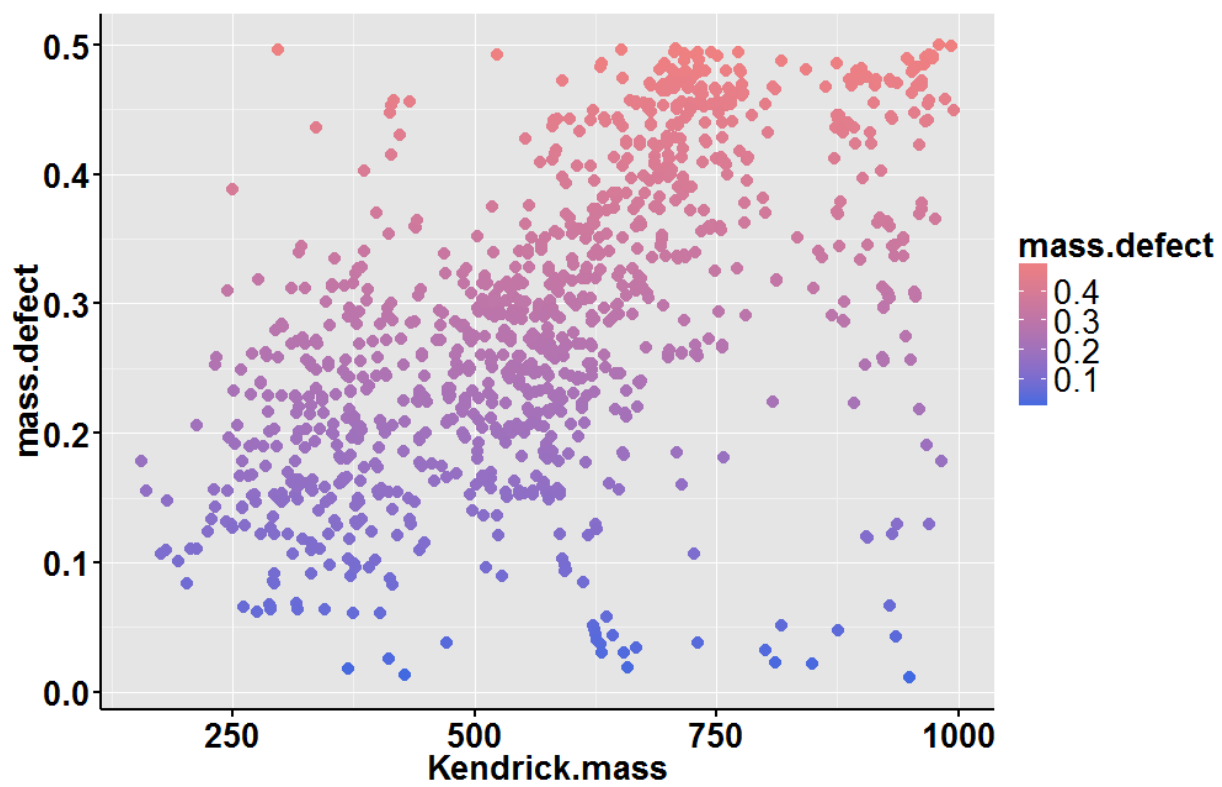


**Figure S4.** Kendrick plot of 1,079 chemicals proposed as potential chemicals causing oxidative stress response in fraction F2.

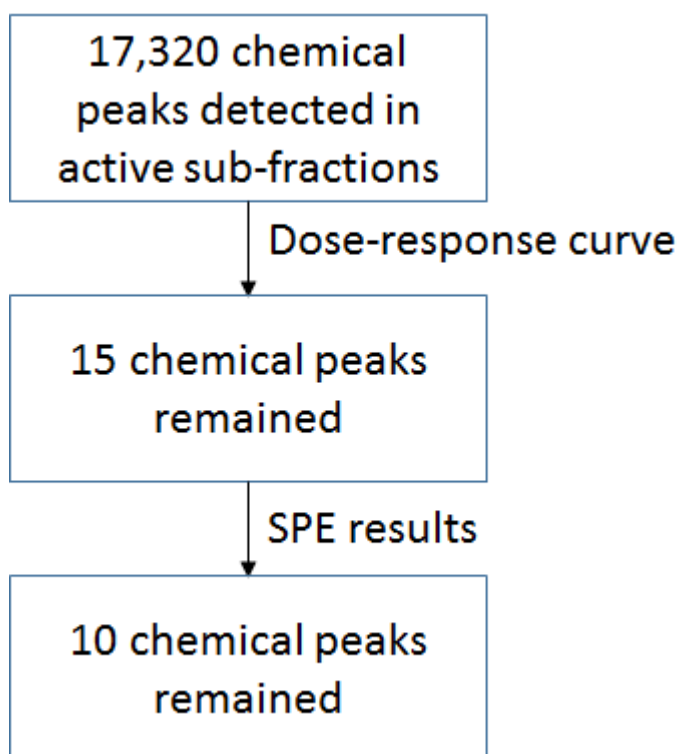


**Figure S5.** Three-step data analysis to identify causative chemicals in HPLC sub-fractions. i) all chemical peaks (17,320) were detected in active sub-fractions, and then were matched across adjoining fractions; ii) potencies for activation of Nrf2 of each fraction were determined, and were used to calculate thresholds to exclude interferences; iii) only those peaks identified by the SPE fractionation method were considered to be potential causative chemicals.

## References

- (1) Smith, C. A.; Want, E. J.; O'Maille, G.; Abagyan, R.; Siuzdak, G., XCMS: Processing mass spectrometry data for metabolite profiling using nonlinear peak alignment, matching, and identification. *Anal. Chem.* **2006**, *78*, (3), 779-787.
- (2) Peng, H.; Chen, C. L.; Saunders, D. M. V.; Sun, J. X.; Tang, S.; Codling, G.; Hecker, M.; Wiseman, S.; Jones, P. D.; Li, A.; Rockne, K. J.; Giesy, J. P., Untargeted identification of organo-bromine compounds in lake sediments by ultrahigh-resolution mass spectrometry with the data-independent precursor isolation and characteristic fragment method. *Anal. Chem.* **2015**, *87*, (20), 10237-10246.